



Spatiotemporal variations of tropospheric SO₂ over China by SCIAMACHY observations during 2004–2009

Xingying Zhang^{a,*}, Jos van Geffen^b, Hong Liao^c, Peng Zhang^a, Sijia Lou^c

^aKey Laboratory of Radiometric Calibration and Validation for Environmental Satellites, China Meteorological Administration (LRCVCS/CMA), National Satellite Meteorological Center, China Meteorological Administration, Beijing 100081, China

^bRoyal Netherlands Meteorological Institute, De Bilt, Netherlands

^cState Key Laboratory of Atmospheric Boundary Layer Physics and Atmospheric Chemistry (LAPC), The Institute of Atmospheric Physics, CAS, Beijing 100029, China

H I G H L I G H T S

- ▶ We validate SCIAMACHY SO₂ data by MAXDOAS in China.
- ▶ Different seasonal variation is found for different energy demand.
- ▶ Tropospheric SO₂ was partly under control from 2007 for the reduction policy.
- ▶ SO₂ decrease in several cities for pollution control for the 2008 Olympic Games.

A R T I C L E I N F O

Article history:

Received 9 April 2012

Received in revised form

4 June 2012

Accepted 4 June 2012

Keywords:

Tropospheric SO₂

SCIAMACHY

Spatiotemporal variations

China

A B S T R A C T

This paper presents results of measurements of tropospheric sulphur dioxide (SO₂) from satellite over China during 2004–2009. SCIAMACHY/ENVISAT SO₂ data products have been validated by ground based remote sensing instrument MAXDOAS in China, and with predictions of the atmospheric model GEOS–Chem. The spatial and temporal distribution of tropospheric SO₂ over China is discussed in this study. The result shows that the SO₂ load over East China is decreasing since strong control for pollution emission in 2007 for preparation of 2008 Olympic Games in China, while the SO₂ load in West China is increasing all the way during 2004–2009, which might reflect that the anthropogenic activity was added to promote the economy development in west of China.

Typical seasonal variation with high pollution levels in winter and low in summer is found in the northwest of China, while the inverse seasonal variation is found for the south of China. The characteristics of tropospheric SO₂ over the major cities in China were explored and found that tropospheric SO₂ was partly under control from 2007 because of the policy from China government for reduction in SO₂ emissions in 2006. And the SO₂ value shows remarkably decrease in most of the major cities after 2007 because strong control for the pollution emission for 2008 Olympic games. Guangzhou city shows high SO₂ pollution levels in summer time, since most of the coal power plants and thermal power industry are located to the south of Guangzhou city and southerly winds dominate during summer time.

© 2012 Elsevier Ltd. All rights reserved.

1. Introduction

Changes in the abundance of sulphur dioxide have an impact on atmospheric chemistry and on the radiation field, and hence on climate. Consequently, global observations of sulphur dioxide are important for atmospheric and climate research. The lifetime of sulphur dioxide molecules in the troposphere is a few days (Eisinger and Burrows, 1998). The amount of SO₂ is highly variable,

above a low background concentration. Clean continental air contains less than 1 ppb of sulphur dioxide, which corresponds to a total column density <0.2 Dobson Units (DU) in a boundary layer of 2 km.

Usually, atmospheric SO₂ was monitored using the accurate but sparse surface SO₂ measurements. But ground stations cannot be distributed equally over the globe or over a large area such as China. Recently satellite observations of the tropospheric SO₂ have become available. The Global Ozone Monitoring Experiment (GOME) on ERS-2 (Eisinger and Burrows, 1998; Khokhar et al., 2005; Thomas et al., 2005), the Scanning Imaging Absorption Spectrometer for Atmospheric Cartography (SCIAMACHY) on ENVISAT (Lee et al., 2008,

* Corresponding author.

E-mail addresses: zxy@cma.gov.cn, zhangxingying@126.com (X. Zhang).

Richter et al., 2006; Loyola et al., 2007), the Ozone Monitoring Instrument (OMI) on EOS/Aura (Krotkov et al., 2006; Carn et al., 2007a,b; Yang et al., 2007), and the GOME-2 instrument on MetOp-A (Loyola et al., 2007) have demonstrated their ability to observe columns of SO₂ in the troposphere using spectroscopic measurements in the ultraviolet. Furthermore, satellite SO₂ data has been used for estimates of the emission from inverse modelling (Lee et al., 2011).

Acid rain and sulphur dioxide (SO₂) pollution in China are very severe problems – ambient concentrations in some regions are several times higher than air quality standards allow – and have a significant impact on human health, ecosystems, and cultural resources. Since 1995 the Chinese government has placed great emphasis on controlling acid rain and SO₂ pollution. Some primary study for SO₂ pollution in China by satellite SO₂ has been explored (Xu et al., 2010). In this study, we report on tropospheric SO₂ data from SCIAMACHY for 2004–2009 over China in detail. Since all data have uncertainties, the results are also compared with other satellite products, in-situ observations data and results from the global 3-D chemistry transfer model GEOS–Chem over China.

2. Methodology and data sources

2.1. SCIAMACHY instrument and SO₂ data retrieval

The SCIAMACHY instrument (Bovensmann et al., 1999) was launched on ENVISAT in a sun-synchronous orbit on March 1st, 2002 and is in nominal operation since August 2002. With a resolution of 60 × 30 km², SCIAMACHY reaches the scale of SO₂ urban plumes for major cities. Such satellite observations, together with infrared satellite observations of tropospheric carbon monoxide (Emmons et al., 2004), nitrogen dioxide (Van der et al., 2006), ozone, other gaseous species, and measurements of aerosols by dedicated instruments (Chu et al., 2003; Wang and Christopher, 2003), offer new perspectives to study air pollution.

Using the Differential Optical Absorption Spectroscopy (DOAS) technique (Platt, 1994), a number of atmospheric trace gases can be retrieved from the spectra. The DOAS technique provides the concentration of a trace gas along a so-called slant column (SC), i.e. along the light path between the satellite and the sun. To convert this into a total or vertical column (VC), an air-mass factor (AMF) is needed: $VC = SC/AMF$. The AMF is computed with a radiative transfer model for a variety of observation modes (viewing angle, position of the Sun, ground albedo, etc.) as well as an a-priori vertical distribution of the trace gas. Since the vertical profile of SO₂ is in general unknown, an assumption has to be made. For the SO₂ data used in this paper, the SO₂ is assumed to be located in a 1-km thick layer centred around 1 km above ground level.

The slant column fit of DOAS also provides an estimate of the error on the SC, $E(SC)$, which encompasses errors in the fit itself and in the measurements. An analysis of the effect of errors in the AMF on the vertical column has not been performed yet (and is in fact very difficult), so that it is not possible to provide a reliable estimate of the error on the VC, $E(VC)$. To have at least a rough estimate of the latter, the error on the SC is simply divided by the AMF: $E(VC) = E(SC)/AMF$.

Monthly average SO₂ data is computed by gridding the VC data on a 0.25 by 0.25° latitude–longitude grid and subsequently performing an average per grid cell, without taking the estimate of the error on the VC into account. As a very rough estimate of the error on the monthly data, the average of the error on the VC, $[E(VC)]_{av}$, is currently provided in the data files. This average should be divided by the square-root of the number of data points in the averaging for each grid cell, to find a more reliable estimate of

the error on the average VC: $E([VC]_{av}) = [E(VC)]_{av}/\sqrt{(N - 1)}$. The number of data points in the averaging varies with latitude due to the geographic coverage of the SCIAMACHY measurements. For the area of interest in this paper, with latitudes between about 20° and 45° North, the number of data points is about 9, so that the average error provided in the data file should be divided by about 3 to find the error on the average vertical column density. (In a future version of the gridded SCIAMACHY SO₂ data, the data files will contain information on the number of points in the averaging.) The detailed SO₂ product information can be found in the website (<http://sacs.aeronomie.be/info/index.php>).

2.2. Ground-based remote sensing data

In order to get a quantitative comparison with the satellite data, the ground-based remote sensing data from a MAXDOAS instrument located on the roof of a building in Beijing, above 40 m, is used. The MAXDOAS instrument is produced by Key Laboratory of Environmental Optical and Technology, Anhui Institute of Optics and Fine Mechanics, Chinese Academy of Sciences. MAXDOAS instruments are highly sensitive to absorbers in the lowest few kilometres of the atmosphere and vertical profile information can be retrieved by combining the measurements with Radiative Transfer Model (RTM) calculations. The potential of the technique for a wide variety of studies of tropospheric trace species and its (few) limitations are discussed elsewhere (Honninger et al., 2004; Lee et al., 2006; Lee et al., 2007; Wang et al., 2006).

2.3. GEOS–Chem model

The GEOS–Chem global 3-D model of tropospheric chemistry (Bey et al., 2001) was used to simulate the SO₂ distribution over China in different seasons. The model (version 4.23; see <http://www-as.harvard.edu/chemistry/trop/geos/index.html>) uses assimilated meteorological data from the NASA Goddard Earth Observing System (GEOS) including winds, convective mass fluxes, mixed layer depths, temperature, precipitation, and surface properties. In this study, GEOS–Chem was used with GEOS–3 data products at 4° × 5° global resolution. GEOS–Chem can also be run at 1° × 1° (and coming soon: 0.5° × 0.667°) resolution in nested grids for both China and North America.

3. Results and discussion

3.1. Validation of the satellite data products

The validation of the data products provided by a satellite instrument against ground-based data is among the most important tasks in any mission. Some validations of satellite SO₂ data from OMI have been done by aircraft data in Northeast of China with the long-term mean value is 0.65 DU with a standard deviation 1.1 DU (Krotkov et al., 2008), while the SCIAMACHY SO₂ data in China has not been validated yet. In this study, the ground-based measurements of SO₂ from the MAXDOAS instrument and GEOS–Chem model have been used for validation.

Fig. 1 presents a quantitative comparison between SCIAMACHY and MAXDOAS data during July to October 2008 in Beijing, which shows that SCIAMACHY data is consistent with the ground-based observations from the MAXDOAS instrument. The linearity regression coefficient is 0.92 and ratio 0.76 ($P < 0.0001$, $N = 19$).

Fig. 2 shows the results of a comparison of satellite data with predictions of the atmospheric model GEOS–Chem in two typical cases: January (high pollution) and July (low pollution), and these show that the distribution of tropospheric SO₂ in July monitored by satellite is very similar to model results. In January, the model result

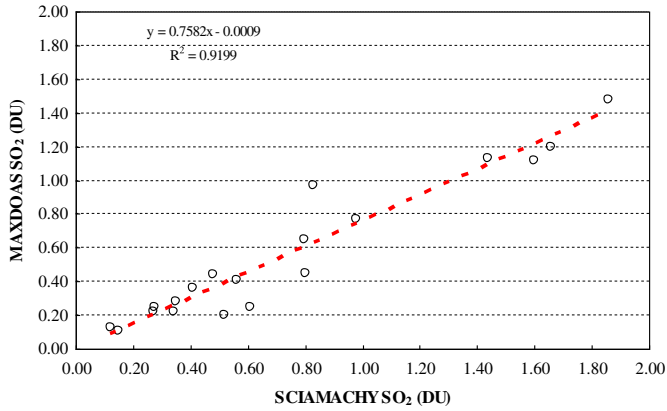


Fig. 1. Correlation of SCIAMACHY and MAXDOAS measurements in Beijing.

is some higher than satellite since the emission source used in the model overestimating SO₂ concentration in East of China in winter season. Fig. 3 presents a quantitative comparison of the data for the east of China (110–120°E, 30–40°N) from satellite and model output, which also shows the model result consists with satellite in summer and a little higher than satellite result in winter. All the

data show a good correspondence with correlation coefficient 0.88 and slope 1.4 ($P < 0.0001$, $N = 12$).

The consistency of SCIAMACHY data with the data from ground based remote sensing are available to give confidence in both the model and SCIAMACHY data over large areas not covered by surface observations. Based on the above primary validation results, the SCIAMACHY data can be used to study the tropospheric SO₂ spatial and temporal distribution and trends over China.

3.2. Spatial and temporal distribution

Using the 2004–2009 SCIAMACHY data, the average distribution of SO₂ over China is shown in the Fig. 4. The highest pollution levels occur in three regions: (1) east of China (110–120°E, 30–40°N); (2) Sichuan basin (104–108°E, 27–31°N); (3) Pearl River Delta region (113–114°E, 22–23°N). The clear region is the (4) west of China (80–100°E, 30–40°N). Fig. 5 exhibits the monthly average tropospheric SO₂ vertical column density over the four areas. The seasonal variation can be seen clearly: that there is low value in summer and high in winter in most of China. But it show inverse seasonal variation in south of China (Pearl River Delta region) and the high pollution occur in summer or fall. Table 1 shows pollution levels averaged from 2004 to 2009, with: East ≈ Sichuan basin > Pearl River delta > West. And the heavy

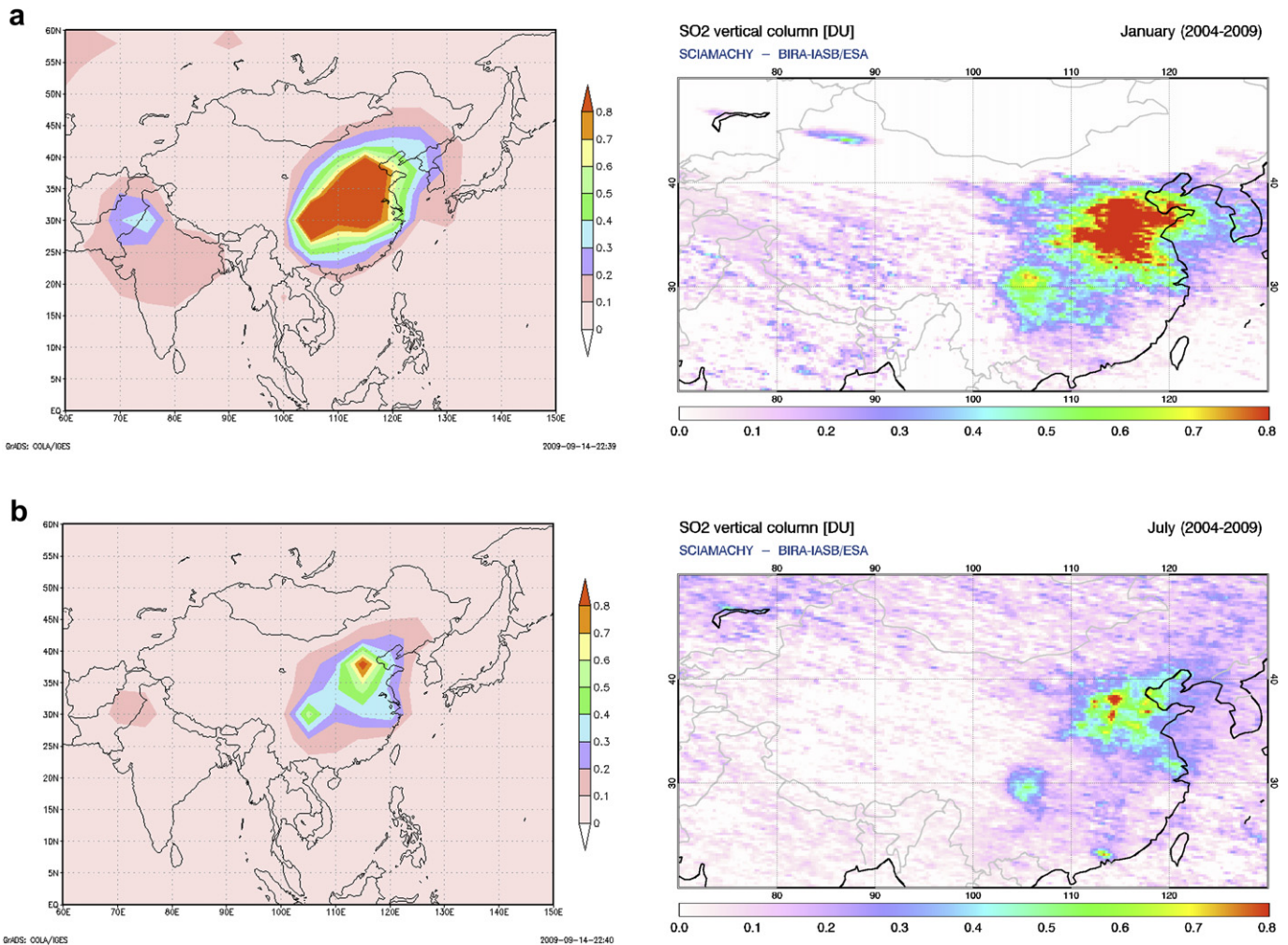


Fig. 2. Comparison of SO₂ concentration in DU from satellite data with the predictions of atmospheric model GEOS–Chem for January and July of averaged over 2004–2009. (a) Jan (b) Jul.

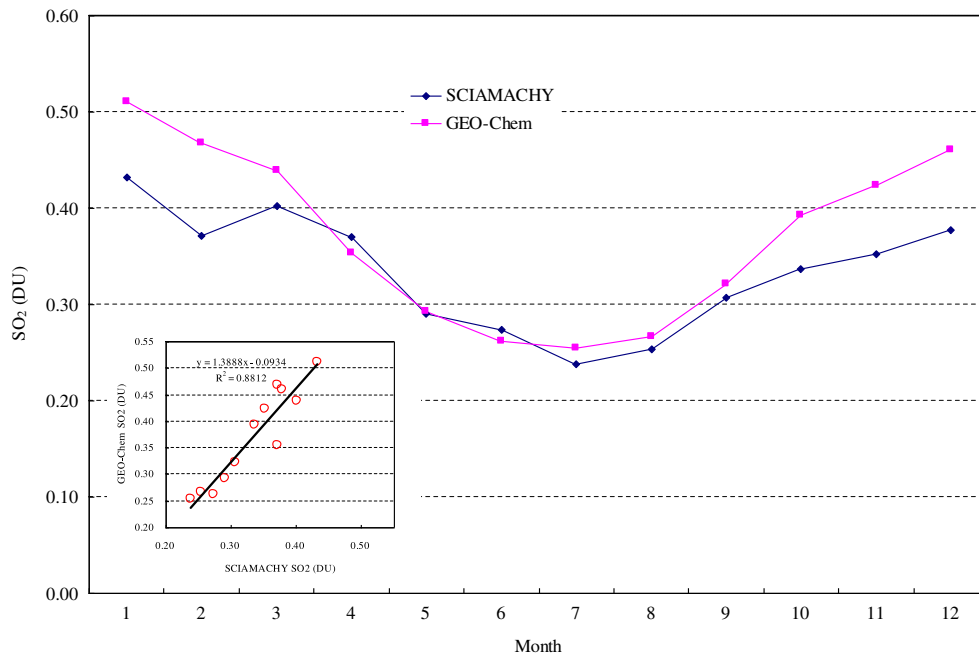


Fig. 3. Correlation of SCIAMACHY monthly average SO₂ data with model results averaged in East of China over 2004–2009.

pollution occurs in east of China (0.34 DU), which is about 4 times the value in west of China (0.09 DU). Fig. 5 also clearly shows that the SO₂ load over East China is decreasing since the strong control for pollution emission in 2007 in preparation of 2008 Olympic Games in China, while the SO₂ load in West China is increasing all the way during 2004–2009, which might reflect

that anthropogenic activity increased due to promoting economic development in west of China. It also can be seen clearly that there is a distinct decrease over the three regions after 2007, except for west of China, that may be caused by the policy of the Chinese government to reduce SO₂ emissions for the Olympic Games in 2008.

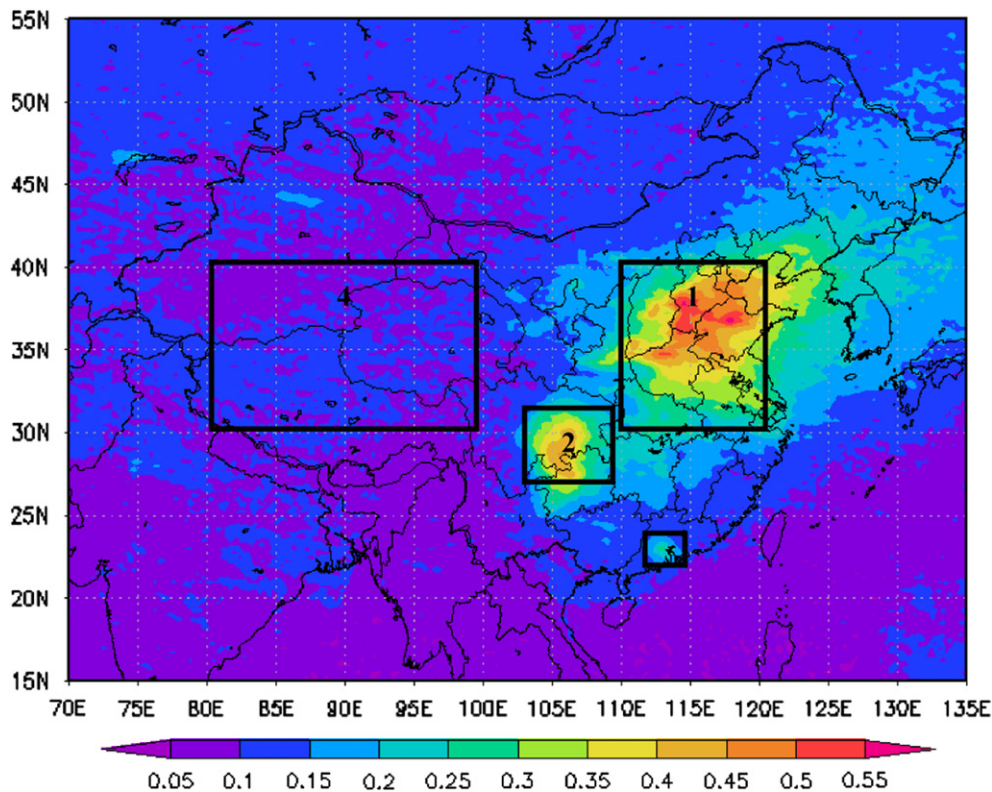


Fig. 4. Tropospheric SO₂ vertical columns in DU averaged during 2004–2009 over China (1) east of China; (2) Sichuan basin; (3) Pearl River Delta region; (4) west of China.

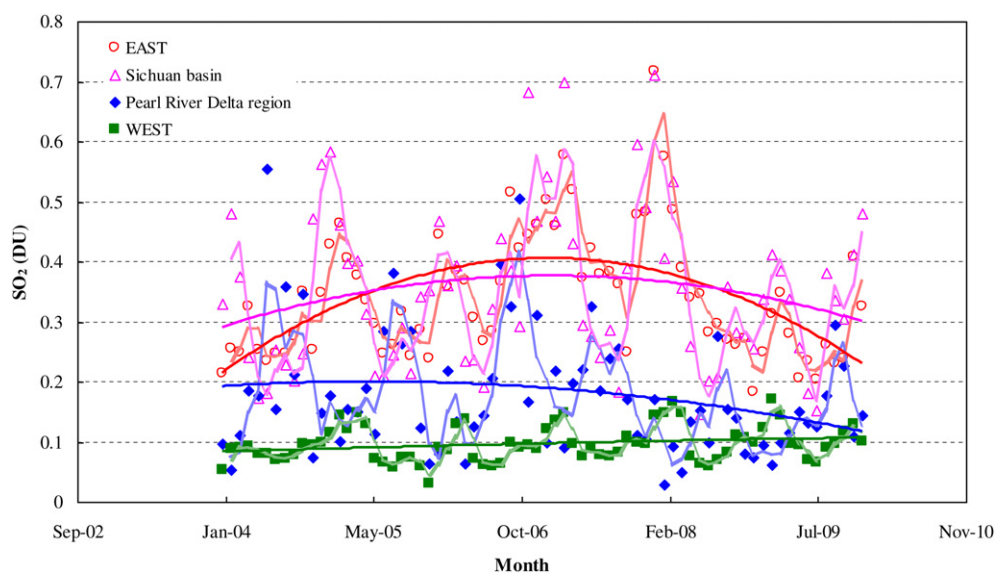


Fig. 5. Monthly variations of tropospheric SO₂ for different regions in China.

3.3. Seasonal variation

Fig. 6 shows the distribution of tropospheric SO₂ over China based on SCIAMACHY data averaged over the period 2004–2009 for the different seasons (spring: MAM, summer: JJA, autumn: SON, winter: DJF). It can be seen clearly that high pollution levels occur in spring and winter in North China. But in South China (Pearl River Delta region), high pollution levels occur during summer and autumn. Fig. 6 also illustrates that the SO₂ pollution seems to move to the Yellow Sea and the Bohai Bay, and even further, to Japan and Korea, during the spring season because of the strong northwest winds and dust storms (Kim and Park, 2001; Ma et al., 2001; Iwasaka et al., 2003; Zhou et al., 1996; Nishikawa et al., 1991).

Fig. 7 shows the monthly variation of the four areas, with their characteristic seasonal variation. The very different seasonal variation for Pearl River delta, with high SO₂ values occurring in summer and autumn, can be seen clearly.

Coal is the main energy source in China and its combustion is the main cause of the increase of atmospheric SO₂ emissions in China. In wintertime, anthropogenic emissions are expected to be higher because of heating of buildings, as shown for China by Streets et al. (2003). This is in particular the case in North China, with its severe winters. In South China much less heating is needed in winter and the main coal consumption in that area comes from coal-fire power plants. During summer, the need for electricity is highest and so the SO₂ pollution is higher in summer than in other seasons in South China (Wang, 2002).

3.4. Characteristics of tropospheric SO₂ over megacities in China

Table 2 lists the year average values of tropospheric SO₂ concentrations for 14 typical major cities in China with a population

of more than one million. It shows that the high SO₂ pollution value averaged over 2004–2009 occur in the cities in North China and low value in the cities in west of China. Shijiazhuang is the heaviest pollution among all the 14 cities.

Fig. 8 exhibits the year average variation of tropospheric SO₂ in those cities. All the cities increased before 2007 since total SO₂ emission in China increased (Lu et al., 2010). Among 14 investigated cities, the SO₂ observably decreased in the 11 cities after 2007. There are only three cities (Taiyuan, Yinchuan and Lanzhou) that show an increase in the SO₂ levels after 2007, which can be found in Table 2 with RED colour.

The reasonable cause is that in 2006, the Chinese State Council issued a Decision on Implementing the Scientific Concept of Development and Stepping up Environmental Protection, which sets the goal for China's environmental protection in the next five to fifteen years, and brings along desulphurization industry with new development opportunities. By the end of 2006, the operated flue gas desulphurization (FGD) unit capacity rose to 53 million kW, starting from 5 million kW at the end of 2000, accounting for some 14% of the thermal power installed capacity; of this 44 million kW was achieved by unit of 100,000 kW and above. Benefit from this policy carried out by Chinese government, is that the SO₂ emissions in China were partly under control from 2006 (Qi et al., 2012). And in order to hold a nice Olympic Games in 2008 Chinese government further reduced the anthropogenic emissions from 2007 by shutting down many Polluting industries, especially in Olympic game cities (Beijing, Shanghai, Shenyang, Qingdao and Hongkong), such as high-emission vehicles were banned from the city's roads and the use of governmental and commercial vehicles were restricted and energy production in major coal-fired power plants was reduced, which cause the SO₂ remarkably decrease after 2007. Especially in Beijing, that traffic within the ring roads was restricted

Table 1
Year average SO₂ value for the four regions in China (2004–2009) (Unit: DU).

Area	Lon/Lat	2004	2005	2006	2007	2008	2009	Average
East	110–120°E, 30–40°N	0.271 ± 0.045	0.326 ± 0.077	0.386 ± 0.075	0.433 ± 0.088	0.368 ± 0.153	0.275 ± 0.062	0.343 ± 0.083
Sichuan Basin	104–108°E, 27–31°N	0.312 ± 0.131	0.335 ± 0.114	0.373 ± 0.134	0.408 ± 0.157	0.333 ± 0.158	0.332 ± 0.096	0.349 ± 0.132
Pearl River delta	113–114°E, 22–23°N	0.206 ± 0.146	0.190 ± 0.094	0.223 ± 0.135	0.185 ± 0.073	0.121 ± 0.066	0.144 ± 0.064	0.178 ± 0.096
West	80–100°E, 30–40°N	0.083 ± 0.013	0.091 ± 0.039	0.090 ± 0.025	0.101 ± 0.024	0.106 ± 0.038	0.108 ± 0.030	0.097 ± 0.028

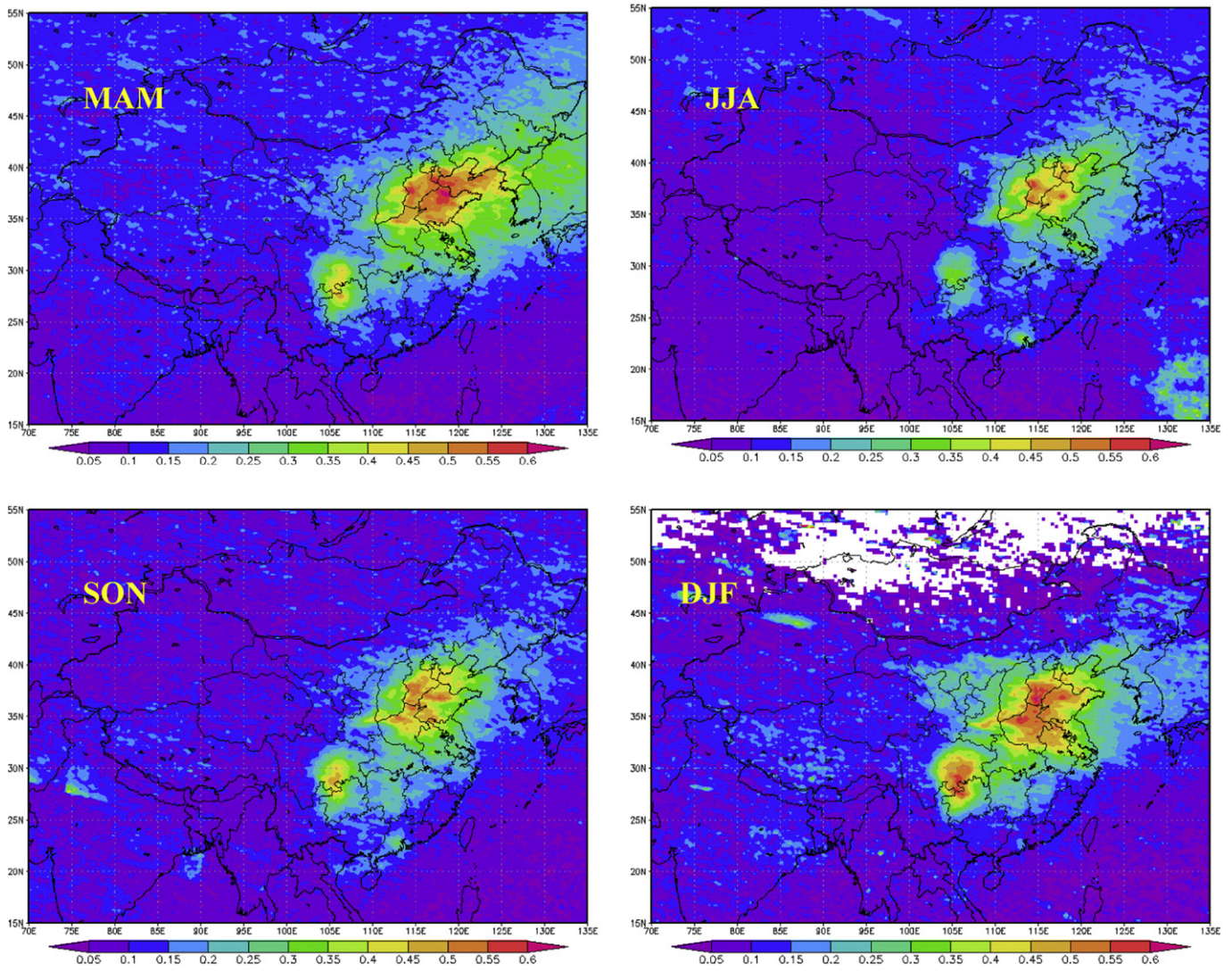


Fig. 6. Distribution of tropospheric SO₂ in DU over China based on SCIAMACHY data of 2004–2009 for the different season.

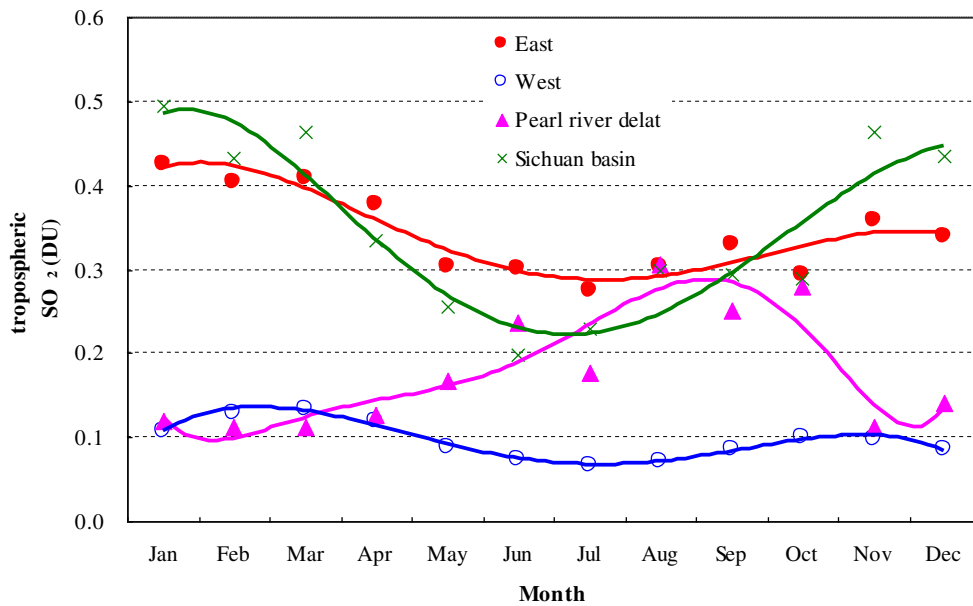


Fig. 7. Monthly variations of tropospheric SO₂ in different areas of China, averaged over 2004–2009.

Table 2Year average SO₂ value for the major cities in China (2004–2009) (Unit: DU).

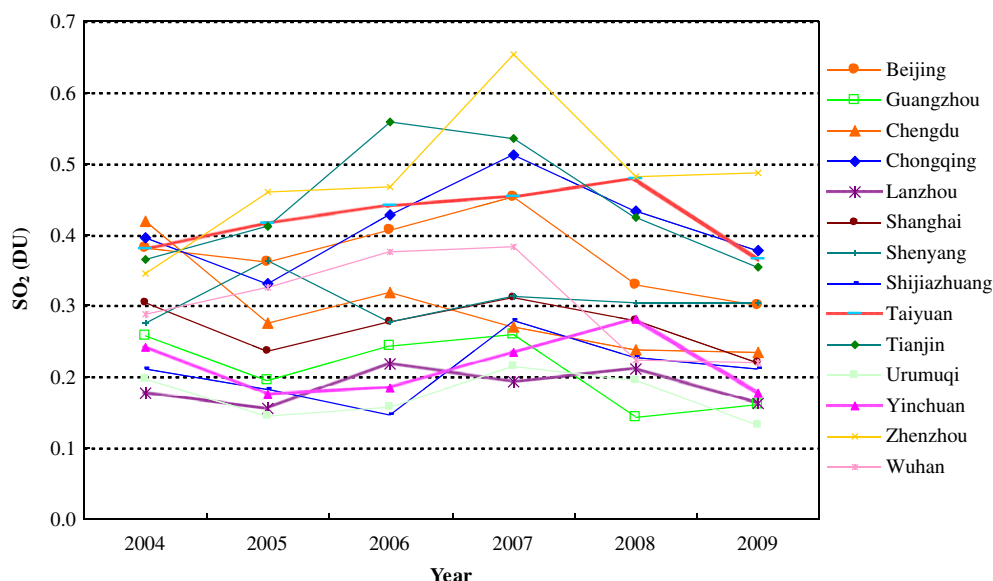
City	Lon/Lat	2004	2005	2006	2007	2008	2009	average
Shijiazhuang	114.48°E, 38.03°N	0.493 ± 0.212	0.454 ± 0.182	0.669 ± 0.147	0.718 ± 0.279	0.521 ± 0.227	0.400 ± 0.211	0.543 ± 0.210
Zhenzhou	113.65°E, 34.77°N	0.346 ± 0.067	0.460 ± 0.108	0.467 ± 0.152	0.653 ± 0.189	0.481 ± 0.297	0.487 ± 0.253	0.482 ± 0.179
Tianjin	117.20°E, 39.13°N	0.366 ± 0.187	0.412 ± 0.142	0.559 ± 0.191	0.536 ± 0.153	0.424 ± 0.190	0.354 ± 0.150	0.442 ± 0.169
Taiyuan	112.53°E, 37.87°N	0.379 ± 0.224	0.416 ± 0.188	0.440 ± 0.136	0.453 ± 0.270	0.478 ± 0.151	0.366 ± 0.172	0.422 ± 0.190
Chongqing	106.54°E, 29.59°N	0.396 ± 0.278	0.331 ± 0.077	0.427 ± 0.152	0.512 ± 0.208	0.433 ± 0.189	0.378 ± 0.150	0.413 ± 0.176
Beijing	116.46°E, 39.92°N	0.381 ± 0.116	0.361 ± 0.168	0.406 ± 0.108	0.453 ± 0.132	0.330 ± 0.152	0.301 ± 0.128	0.372 ± 0.134
Shenyang	123.38°E, 41.80°N	0.276 ± 0.180	0.364 ± 0.154	0.278 ± 0.104	0.314 ± 0.192	0.305 ± 0.151	0.304 ± 0.099	0.307 ± 0.295
Wuhan	114.32°E, 30.52°N	0.288 ± 0.091	0.325 ± 0.113	0.376 ± 0.137	0.384 ± 0.131	0.223 ± 0.099	0.221 ± 0.106	0.303 ± 0.113
Chengdu	104.06°E, 30.67°N	0.419 ± 0.241	0.276 ± 0.118	0.319 ± 0.121	0.270 ± 0.121	0.238 ± 0.187	0.235 ± 0.132	0.293 ± 0.153
Shanghai	121.48°E, 31.22°N	0.305 ± 0.150	0.236 ± 0.097	0.277 ± 0.104	0.311 ± 0.158	0.279 ± 0.118	0.221 ± 0.077	0.272 ± 0.117
Yinchuan	106.27°E, 38.47°N	0.241 ± 0.181	0.175 ± 0.084	0.184 ± 0.137	0.235 ± 0.162	0.281 ± 0.225	0.177 ± 0.122	0.216 ± 0.152
Guangzhou	113.23°E, 23.16°N	0.258 ± 0.186	0.196 ± 0.100	0.243 ± 0.106	0.260 ± 0.097	0.143 ± 0.088	0.162 ± 0.093	0.210 ± 0.112
Lanzhou	103.73°E, 36.03°N	0.178 ± 0.119	0.155 ± 0.091	0.218 ± 0.147	0.194 ± 0.106	0.212 ± 0.147	0.163 ± 0.128	0.187 ± 0.123
Urumuqi	87.68°E, 43.70°N	0.197 ± 0.192	0.145 ± 0.109	0.158 ± 0.097	0.214 ± 0.140	0.195 ± 0.174	0.132 ± 0.108	0.174 ± 0.137

to cars with even number plates on even days and with odd numbers on odd days (from 20 July). 300,000 high-emission vehicles were banned from the city's roads (1 July) and the use of governmental and commercial vehicles was restricted (by 50% from 23 June; by 70% after 1 July). Access to specific roads (the "Olympic Lanes") was prohibited for other than Olympic related traffic. Public transport capacity was increased with the introduction of new metro and bus lines. Polluting industry was shut down temporarily (20 July) or rebuilt outside Beijing. Energy production in major coal-fired power plants was reduced by 30% (20 July). All construction activities were put on hold (20 July). And now the car in Beijing is still restricted for one day each week. Fig. 9 clearly shows that the SO₂ during Jul to Dec in 2008 is lower than the average from other years at the same period. In-situ measurement also shows a significant decrease from period before to after the control measures for the 2008 Olympic Games (Lin et al., 2012).

Since surrounding areas can contribute significantly to air pollution in Olympic game cities (Streets et al., 2007), similar measures have been taken in the surrounding areas, such as Heibei and Henan province, which are adjacent to Beijing and Qingdao respectively. So the SO₂ value for Shijiazhuang city in Hebei province and Zhenzhou city in Henan province show distinctly decrease from 2007 (see Fig. 8).

Some cities, such as Taiyuan, Yinchuan and Lanzhou, showed an increase in tropospheric SO₂ due to lack of industrial standards, laws & regulations, a lot of medium- and small-scale enterprises (the number of which increased from 2 in 2001 to 200 in 2006) compete maliciously in the market by price war, resulting in a steep decline of the gross margin of the desulphurization industry. Moreover, Taiyuan is one of the main coal mining areas in China. So those three cities still show an increase after 2007.

Fig. 10 shows the monthly variations of tropospheric SO₂ in some typical megacities of China. It can be seen clearly that cities located in the north of China show lowest SO₂ pollution levels in summer because of prominent anthropogenic activities and meteorological conditions (Chen et al., 2011). But the highest SO₂ value doesn't occur in December and January in Tianjin and Shanghai because of less effective data retrieved. In Guangzhou, the seasonal characteristic is reversed and high SO₂ pollution occurs in summer. Because Guangzhou is located in the south of China, there is little or no heating needed in winter and the main coal consumers are coal power plants. During summer, the need for electricity is the highest of the whole year and so the SO₂ pollution is higher in summer than in other seasons. Xie and Chen, 2003 showed that most of the coal power plants and thermal power industry are located to the south of Guangzhou city. The higher SO₂

**Fig. 8.** Year variations of tropospheric SO₂ in 14 major cities of China.

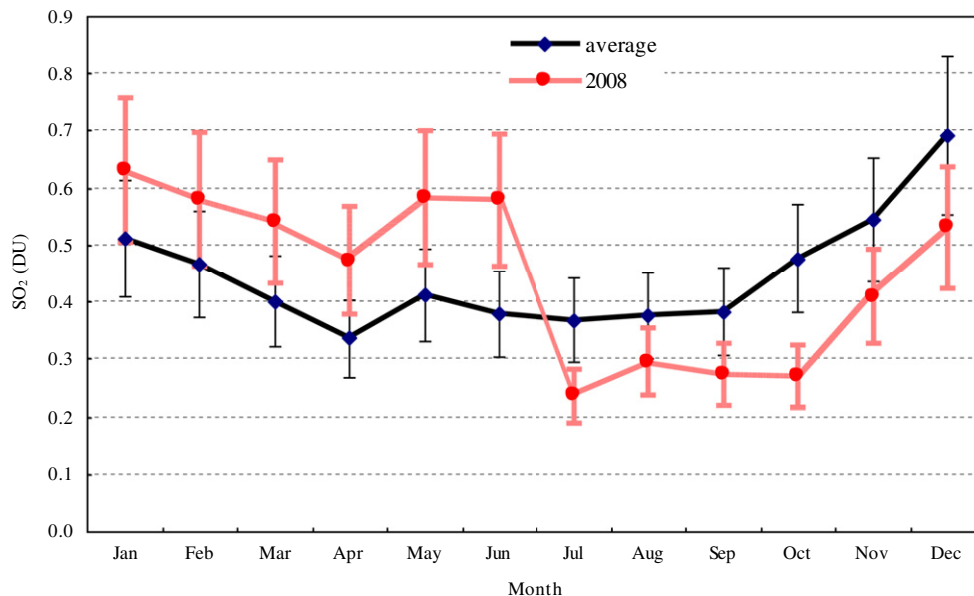


Fig. 9. Monthly variations of tropospheric SO₂ in Beijing.

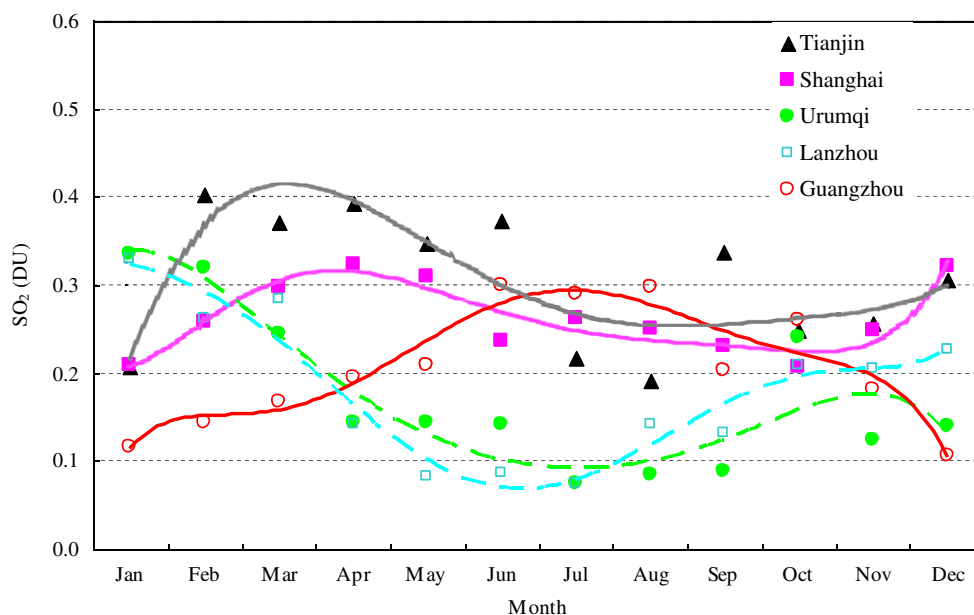


Fig. 10. Monthly variations of tropospheric SO₂ in major cities of China, averaged over 2004–2009.

pollution in summer is caused by the southerly winds which then dominate the city, while in winter the main wind direction is from the north.

4. Conclusion

The tropospheric SO₂ columns measured by SCIAMACHY during 2004–2009 have been used to study the spatial and temporal distribution of tropospheric SO₂ over China. The main results of this study can be summarised as follows.

(1) Validation of the SCIAMACHY SO₂ data shows that there is consistency between SCIAMACHY and MAXDOAS data, and results from GEOS–Chem. SCIAMACHY data can therefore be

used to study the spatial and temporal distribution of tropospheric SO₂ spatial and trends therein for China.

- (2) The geographic annual average distribution of tropospheric SO₂ over China was studied. Heavy SO₂ pollution occurs in the east of China and Sichuan basin because of prominent anthropogenic activities. A low tropospheric SO₂ column exists in western China because there is less anthropogenic activity.
- (3) A typical seasonal variation with high pollution in winter and low in summer in the northwest of China has been found, while the inverse seasonal characteristic appears in the south of China for the energy demand and meteorological conditions.
- (4) The characteristics of tropospheric SO₂ over the major cities in China were explored and the results show that tropospheric SO₂ was partly under control from 2007 because of the policy

from China government for reduction in SO₂ emissions in 2006. And the SO₂ value shows remarkably decrease in most of major cities after 2007 because strong control for the pollution emission for 2008 Olympic games in China.

Acknowledgement

This work was supported by National Natural Science Funds of China (Grant No. 40905056), Special Fund for Meteorological Research in the Public Interest (Grant No. GYHY201106045), the fund from State Key Laboratory of Atmospheric Boundary Layer Physics and Atmospheric Chemistry (Grant No. LAPC-KF-2008-11), and the European Union project “AMFIC” (Grant No. FP6-2005-Space-1).

References

- Bey, I., Jacob, D.J., Yantosca, R.M., Logan, J.A., Field, B., Fiore, A.M., Li, Q., Liu, H., Mickley, L.J., Schultz, M., 2001. Global modeling of tropospheric chemistry with assimilated meteorology: model description and evaluation. *J. Geophys. Res.* 106, 23,073–23,096.
- Bovensmann, H., Burrows, J.P., Buchwitz, M., Frerick, J., Noël, S., Rozanov, V.V., Chance, K.V., Goede, A.P.H., 1999. SCIAMACHY: mission objectives and measurement modes. *J. Atmos. Sci.* 56, 127–150.
- Carn, S.A., Krotkov, N.A., Yang, K., Hoff, R.M., Prata, A.J., Krueger, A.J., Loughlin, S.C., Levelt, P.F., 2007a. Extended observations of volcanic SO₂ and sulfate aerosol in the stratosphere. *Atmos. Chem. Phys. Discuss.* 7, 2857–2871.
- Carn, S.A., Krotkov, N.A., Krueger, A.J., Yang, K., Levelt, P.F., 2007b. Sulfur dioxide emissions from Peruvian copper smelters detected by the Ozone Monitoring Instrument. *Geophys. Res. Lett.* 34, L09801. <http://dx.doi.org/10.1029/2006GL029020>.
- Chen, S., Li, N., Hiroshi, Y., Guan, J., Mark, D.L., 2011. Statistical analyses on winter energy consumption characteristics of residential buildings in some cities of China. *Energy Buildings* 43, 1063–1070.
- Chu, D.A., Kaufman, Y.J., Zibordi, G., Chern, J.D., Mao, J., Li, C., Holben, B.N., 2003. Global monitoring of air pollution over land from EOS-Terra MODIS. *J. Geophys. Res.* 108 (D21), 4661. <http://dx.doi.org/10.1029/2002JD003179>.
- Eisinger, M., Burrows, J.P., 1998. Tropospheric sulfur dioxide observed by the ERS-2 GOME instrument. *Geophys. Res. Lett.* 25, 4177–4180.
- Emmons, L.K., Deeter, M.N., Gille, J.C., Edwards, D.P., 2004. Validation of measurements of pollution in the troposphere (MOPITT) CO retrievals with aircraft in situ profiles. *J. Geophys. Res.* 109 (D3), D03309. <http://dx.doi.org/10.1029/2003JD004101>.
- Honninger, G., von Friedeburg, C., Platt, U., 2004. Multi axis differential optical absorption spectroscopy (MAX-DOAS). *Atmos. Chem. Phys.* 4, 231–254.
- Iwasaka, Y., Shi, G.-Y., Shen, Z., Kim, Y.S., Trochkin, D., Matsuki, A., Zhang, D., Shibata, T., Nagatani, M., Nakata, H., 2003. Nature of atmospheric aerosols over the desert areas in the Asian continent: chemical state and number concentration of particles measured at Dunhuang, China. *Water, Air, Soil Pollut.: Focus* 3 (2), 129–145.
- Khokhar, M.F., Frankenberg, C., Van Roozendael, M., Beirle, S., Kuhl, S., Richter, A., Platt, U., Wagner, T., 2005. Satellite observations of atmospheric SO₂ from volcanic eruptions during the time-period of 1996–2002. *Adv. Space Res.* 36, 879–887.
- Kim, Byung-Gon, Park, Soon-Ung, 2001. Transport and evolution of a winter-time Yellow sand observed in Korea. *Atmos. Environ.* 35, 3191–3201.
- Krotkov, N.A., Carn, S.A., Krueger, A.J., Bhartia, P.K., Yang, K., May 2006. Band residual difference algorithm for retrieval of SO₂ from the Aura Ozone Monitoring Instrument (OMI). *IEEE Trans. Geosci. Remote Sens.* 44 (5), 1259–1266.
- Krotkov, N.A., McClure, B., Dickerson, R.R., Carn, S.A., Li, C., Bhartia, P.K., Yang, K., Krueger, A.J., Li, Z., Levelt, P.F., Chen, H., Wang, P., Lu, D., 2008. Validation of SO₂ retrievals from the ozone monitoring instrument over NE China. *J. Geophys. Res.* 113, D16S40. <http://dx.doi.org/10.1029/2007JD008818>.
- Lee, Chulkyu, Lee, Hanlim, Kim, Young J., Choi, Byeong-Chul, 2006. MAX-DOAS measurements of ClO, SO₂ and NO₂ in the Mid-latitude Coastal Boundary Layer, The 6th symposium on Advanced Environmental Monitoring, June 27–30, 2006, Heidelberg, Germany.
- Lee, Hanlim, Kim, Young J., Lee, Chulkyu, Kim, Yeo Sook, 2007. Remote Measurement of Atmospheric Trace Gases and Aerosol Using Multi-Axis Differential Optical Absorption Spectroscopy (MAX-DOAS) and Imaging DOAS (I-DOAS) Techniques, The 10th International Conference on Atmospheric Sciences and Applications to Air Quality, May 14–16, 2007, Hong Kong, China.
- Lee, C., Richter, A., Weber, M., Burrows, J.P., 2008. SO₂ Retrieval from SCIAMACHY using the Weighting Function DOAS (WFDOAS) technique: comparison with Standard DOAS retrieval. *Atmos. Chem. Phys.* 8, 6137–6145.
- Lee, C., Martin, R.V., van Donkelaar, A., Lee, H., Dickerson, R.R., Hains, J.C., Krotkov, N., Richter, A., Vinnikov, K., Schwab, J.J., 2011. SO₂ emissions and lifetimes: estimates from inverse modeling using in situ and global, space-based (SCIAMACHY and OMI) observations. *J. Geophys. Res.* 116, D06304. <http://dx.doi.org/10.1029/2010JD014758>.
- Lin, W., Xu, X., Ma, Z., Zhao, H., Liu, X., 2012. Characteristics and recent trends of surface SO₂ at urban, rural, and background sites in North China: effectiveness of control measures. *J. Environ. Sci.* 24 (1), 34–49.
- Loyola, D., Van Geffen, J., Valks, P., Erbertseder, T., Van Roozendael, M., Thomas, W., Zimmer, W., Wißkirchen, K., 2007. Satellite-based detection of volcanic sulphur dioxide from recent eruptions in Central and South America. *Adv. Geosci.* 14, 35–40.
- Lu, Z., Streets, D.G., Zhang, Q., Wang, S., Carmichael, G.R., Cheng, Y.F., Wei, C., Chin, M., Diehl, T., Tan, Q., 2010. Sulfur dioxide emissions in China and sulfur trends in East Asia since 2000. *Atmos. Chem. Phys.* 10, 6311–6331.
- Ma, Chang-Jin, Kasahara, Mikio, Höller, Robert, Tomihiro, Kamiya, 2001. Characteristics of single particles sampled in Japan during the Asian dust-storm period. *Atmos. Environ.* 35, 2707–2714.
- Nishikawa, Masataka, Kanamori, Satoru, Kanamori, Nobuko, Mizoguchi, Tsuguo, 1991. Kosa aerosol as eolian carrier of anthropogenic material. *Sci. Total Environ.* 107, 13–27.
- Platt, U., 1994. Differential Optical Absorption Spectroscopy (DOAS). In: Sigrist, M.W. (Ed.), *Air Monitoring by Spectroscopic Techniques*. Chemical Analysis Series, vol. 127. John Wiley & Sons, New York.
- Qi, H., Lin, W., Xu, X., Yu, X., Ma, Q., 2012. Significant downward trend of SO₂ observed from 2005 to 2010 at a background station in the Yangtze Delta region, China. *Sci. China Chem.* <http://dx.doi.org/10.1007/s11430-011-4205-2>.
- Richter, A., Wittrock, F., Burrows, J.P., 2006. SO₂ measurements with SCIAMACHY. In: *Proceedings of the First Conference on Atmospheric Science*, 8–12 May 2006. ESA publication SP-628, Frascati, Italy.
- Streets, D.G., Bond, T.C., Carmichael, G.R., et al., 2003. An inventory of gaseous and primary aerosol emissions in Asia in the year 2000. *J. Geophys. Res.* 108 (D21), 8809. <http://dx.doi.org/10.1029/2002JD003093>.
- Streets, D.G., Fu, J.S., Jang, C.J., Hao, J., He, K., Tang, X., Zhang, Y., Wang, Z., Li, Z., Zhang, Q., Wang, L., Wang, B., Yu, C., January 2007. Air quality during the 2008 Beijing Olympic Games. *Atmos. Environ.* ISSN: 1352-2310 41 (3). ISSN: 1352-2310, 480–492. <http://dx.doi.org/10.1016/j.atmosenv.2006.08.046>.
- Thomas, W., Erbertseder, T., Ruppert, T., Van Roozendael, M., Verdebout, J., Balis, D., Meleti, C., Zerefos, C., 2005. On the retrieval of volcanic sulfur dioxide emissions from GOME backscatter measurements. *J. Atmos. Chem.* 50, 295–320. <http://dx.doi.org/10.1007/s10874-005-5079-5>.
- Van der Aar, J., Peters, D.H.M.U., Eskes, H., Boersma, K.F., Van Roozendael, M., De Smedt, I., Kelder, H.M., 2006. Detection of the trend and seasonal variation in tropospheric NO₂ over China. *J. Geophys. Res.* 111, D12317. <http://dx.doi.org/10.1029/2005JD006594>.
- Wang, Zhi xuan, 2002. Integrated countermeasures and suggestions to SO₂ emission control of thermal power plants in China. *Electricity* 13 (1), 23–26.
- Wang, J., Christopher, S.A., 2003. Intercomparison between satellite derived aerosol optical thickness and PM_{2.5} mass: implications for air quality studies. *Geophys. Res. Lett.* 30 (21), 2095. <http://dx.doi.org/10.1029/2003GL018174>.
- Wang, P., Richter, A., Bruns, M., Burrows, J.P., Scheele, R., Junkermann, W., Heue, K.-P., Wagner, T., Platt, U., Pundt, I., 2006. Airborne multi-axis DOAS measurements of tropospheric SO₂ plumes in the Po-valley, Italy. *Atmos. Chem. Phys.* 6, 329–338.
- Xie, M., Chen, Y.S., 2003. SO₂ pollution of Guangzhou in recent years: its characteristics and sources. *Environ. Science Technol.* 26 (2), 18–21 (in Chinese).
- Xu X., Jiang H., Wang Y., Zhang X., 2010. Temporal-spatial Variations of Tropospheric SO₂ over China Using SCIAMACHY Satellite Observations, *Geoinformatics*, 18–20 June 2010, 18th International Conference, p. 1–5.
- Yang, K., Krotkov, N.A., Krueger, A.J., Carn, S.A., Bhartia, P.K., Levelt, P.F., 2007. Retrieval of large volcanic SO₂ columns from the Aura ozone monitoring instrument: comparison and limitations. *J. Geophys. Res.* 112, D24S43. <http://dx.doi.org/10.1029/2007JD008825>.
- Zhou, M., Okada, K., Qian, F., Wu, P.M., Su, L., Casareto, B.E., Shimohara, T., 1996. Characteristics of dust-storm particles and their long-range transport from China to Japan – case studies in April 1993. *Atmos. Res.* 40, 19–31.